

# UC San Diego

## UC San Diego Previously Published Works

### Title

Traditional Chinese medicine herbal mixture LQ arrests FUCCI-expressing HeLa cells in G0/G1 phase in 2D plastic, 2.5D Matrigel®, and 3D Gelfoam® culture visualized with FUCCI imaging

### Permalink

<https://escholarship.org/uc/item/9bs4b521>

### Journal

Oncotarget, 6(7)

### ISSN

1949-2553

### Authors

Zhang, Lei  
Wu, Chengyu  
Bouvet, Michael  
et al.

### Publication Date

2015-03-10

### DOI

10.18632/oncotarget.2983

Peer reviewed

# Traditional Chinese medicine herbal mixture LQ arrests FUCCI-expressing HeLa cells in G<sub>0</sub>/G<sub>1</sub> phase in 2D plastic, 2.5D Matrigel®, and 3D Gelfoam® culture visualized with FUCCI imaging

Lei Zhang<sup>1,\*</sup>, Chengyu Wu<sup>2,\*</sup>, Michael Bouvet<sup>3</sup>, Shuya Yano<sup>1,3,4</sup>, Robert M. Hoffman<sup>1,3</sup>

<sup>1</sup>AntiCancer, Inc., San Diego, CA, USA

<sup>2</sup>Department of Traditional Chinese Medicine Diagnostics, Nanjing University of Traditional Chinese Medicine, Nanjing, China

<sup>3</sup>Department of Surgery, University of California at San Diego, San Diego, CA, USA

<sup>4</sup>Department of Gastroenterological Surgery, Okayama University Graduate School of Medicine, Dentistry and Pharmaceutical Sciences, Okayama, Japan

\*These authors have contributed equally to this work

## Correspondence to:

Robert M. Hoffman, e-mail: all@anticancer.com

Chengyu Wu, e-mail: chengyu720@yahoo.com.cn

**Keywords:** TCM, herbal mixture, LQ, paclitaxel, FUCCI

**Received:** November 20, 2014

**Accepted:** December 20, 2014

**Published:** March 12, 2015

## ABSTRACT

**We used the fluorescence ubiquitination-based cell cycle indicator (FUCCI) to monitor cell cycle arrest after treatment of FUCCI-expressing HeLa cells (FUCCI-HeLa) with a traditional Chinese medicine (TCM) herbal mixture LQ, previously shown to have anti-tumor and anti-metastatic activity in mouse models. Paclitaxel was used as the positive control. In 2D monolayer culture, the untreated control had approximately 45% of the cells in S/G<sub>2</sub>/M phase. In contrast, the LQ-treated cells (9 mg/ml) were mostly in the G<sub>0</sub>/G<sub>1</sub> (>90%) after 72 hours. After treatment with paclitaxel (0.01 μm), for 72 hours, 95% of the cells were in S/G<sub>2</sub>/M. In 2.5D Matrigel® culture, the colonies in the untreated control group had 40% of the cells in S/G<sub>2</sub>/M. LQ arrested the cells in G<sub>0</sub>/G<sub>1</sub> after 72 hours. Paclitaxel arrested almost all the cells in S/G<sub>2</sub>/M after 72 hours. In 3D Gelfoam® culture, the untreated control culture had approximately 45% of cells in G<sub>2</sub>/M. In contrast, the LQ-treated cells were mostly in G<sub>0</sub>/G<sub>1</sub> phase (>80%) after 72 hours treatment. Paclitaxel resulted in 90% of the cells arrested in S/G<sub>2</sub>/M after 72 hours. The present report suggests the non-toxic LQ has potential to maintain cancers in a quiescent state for long periods of time.**

## INTRODUCTION

Traditional Chinese medicine (TCM) compositions usually comprise multiple herbs and many components may be necessary for efficacy. We previously compared the efficacy of the TCM herbal mixture LQ against lung cancer in mouse models with doxorubicin (DOX) and cyclophosphamide (CTX). LQ was effective against primary and metastatic lung cancer without weight loss and organ toxicity. In contrast, although CTX and DOX had efficacy in the lung cancer models, they caused significant weight loss and organ toxicity. LQ also had anti-angiogenic activity as observed in lung tumors growing in nestin-driven

green fluorescent protein (ND-GFP) transgenic nude mice, which selectively express GFP in nascent blood vessels. LQ also increased survival of tumor-bearing mice, comparable to DOX. *In vitro*, lung cancer cells were killed by LQ, comparable to cisplatin. LQ selectively killed cancer cell lines compared to normal cell strains unlike cytotoxic drugs which killed both similarly [1].

In another previous study, LQ significantly inhibited pancreatic cancer tumor growth and metastasis in orthotopic models with no overt toxicity. LQ also increased survival of tumor-bearing mice. The antitumor efficacy of LQ was comparable with gemcitabine (GEM), but with less toxicity than GEM [2].

Sakaue-Sawano et al. [3] developed a fluorescence ubiquitination-based cell-cycle indicator (FUCCI). With FUCCI,  $G_0/G_1$  cells express an orange-red fluorescent protein and  $S/G_2/M$  cells express a yellow-green fluorescent protein. We previously determined with FUCCI imaging the cell-cycle phase of invading cancer cells [4] and the spatial-temporal cell-cycle phase distribution of cancer cells within tumors before and after chemotherapy [5].

The present report uses FUCCI imaging to demonstrate the effect of LQ on the cell cycle arrest of HeLa cells.

## RESULTS AND DISCUSSION

### Effect of LQ or paclitaxel on the cell-cycle phase distribution of FUCCI-HeLa cells growing in 2D culture

Untreated control HeLa-FUCCI cells exhibited a combination of orange-red and yellow-green nuclei. Approximately 60% of the cells were in  $S/G_2/M$  and 40% in  $G_0/G_1$ . The cultures were approaching confluence. After treatment with LQ (9 mg/ml) for 72 hours, the HeLa-FUCCI cells were almost all arrested in  $G_0/G_1$ . Only approximately 5% were in  $S/G_2/M$  phases and the remainder in  $G_0/G_1$ . After treatment with paclitaxel (0.01  $\mu$ M), for 72 hours, approximately 5% of the cells were in  $G_0/G_1$  with the rest of the cells arrested in  $S/G_2/M$ . Almost all the paclitaxel-treated cells fluoresced yellow-green, in contrast to LQ-treated cells, which almost all fluoresced orange-red (Figure 1).

### Effect of LQ or paclitaxel on the cell-cycle phase distribution of FUCCI-HeLa cells growing in 2.5D Matrigel culture

The untreated control cells exhibited a combination of orange-red and yellow-green nuclei with the cells growing in colonies. Approximately 50% of the cells were in  $S/G_2/M$  and 50% in  $G_0/G_1$ . LQ (9 mg/ml) had a similar effect in Matrigel as on plastic, with most of the cells arresting in  $G_0/G_1$  and only 10% in  $S/G_2/M$  after 72 hours of treatment. Paclitaxel (0.01  $\mu$ M) in 2.5 D Matrigel culture, as in 2D culture, arrested the cells almost all in  $S/G_2/M$  after 72 hours treatment (Figure 2).

### Effect of LQ or paclitaxel on the cell-cycle phase distribution of FUCCI-HeLa cells growing in Gelfoam® histoculture

Control cells in Gelfoam® histoculture exhibited a combination of orange-red and yellow-green nuclei. Approximately 60% of the cells were in  $S/G_2/M$  with almost 20% in M, a surprisingly large percentage. Treatment with LQ (9 mg/ml) for 72 hours resulted in over 80% of the cells being arrested in  $G_0/G_1$ , similar to 2 D plastic culture

and 2.5 D Matrigel culture. Paclitaxel (0.01  $\mu$ M) resulted in 90% of the cells arrested in  $S/G_2/M$ , as in 2D and 2.5D culture, after 72 hours treatment (Figure 3).

Methionine deprivation, either by nutritional means or recombinant methioninase (rMETase) treatment, selectively trapped cancer cells in  $S/G_2$  [6, 7]. Excess thymidine, or its analogs, arrested cancer cells in S-phase [8–10]. The calcium-channel blocker mibefradil arrested glioblastoma cells at the  $G_1/S$  checkpoint [11]. Statins, such as Lovastatin, can arrest cancer cells in  $G_0/G_1$  [12, 13]. PDO332991, a pyridopyrimidine-selective inhibitor of cyclin-dependent kinases 4 and 6, induced early- $G_0/G_1$  arrest in various cancer cell types, including melanoma and breast cancer *in vitro*, and in cancer xenograft models. RO-3306, also a cyclin-dependent kinase inhibitor, reversibly arrested 95% of treated cells in  $G_2$  phase [14–17]. Since LQ has been shown to be non-toxic, it has potential to maintain cancers in a quiescent state for long periods of time.

Previously-developed concepts and strategies of highly-selective tumor targeting [18–29] can take advantage of cell-cycle imaging of cancer cells and  $G_0/G_1$  blockage by LQ, described in the present report.

## MATERIALS AND METHODS

### Cell line

FUCCI-expressing HeLa cells were grown in DMEM supplemented with 10% fetal bovine serum.

### Establishment of HeLa cells stably transfected with FUCCI plasmids

Plasmids expressing mKO2-hCdt1 (yellow-green fluorescent protein) and mAG-hGem (orange-red fluorescent protein) (Medical and Biological Laboratory, Nagoya, Japan) [3], were transfected into HeLa cells with Lipofectamine™ LTX (Invitrogen).

### Two-dimensional monolayer culture

FUCCI-expressing HeLa cells were grown as monolayer in 35 mm dishes in DMEM supplemented with 10% fetal bovine serum.

### Matrigel (2.5 D culture)

Matrigel (100  $\mu$ l/chamber well) was pipetted into the center of the well and then allowed to spread evenly for 15–30 minutes at 37°C in order for the Matrigel to solidify. FUCCI-expressing HeLa cells ( $4 \times 10^4$ ) were grown for 4 days in Matrigel and DMEM supplemented with 10% fetal bovine serum.

### Gelfoam® (3D culture)

Sterilized Gelfoam® was cut and placed in wells. The Gelfoam® was hydrated in DMEM medium for

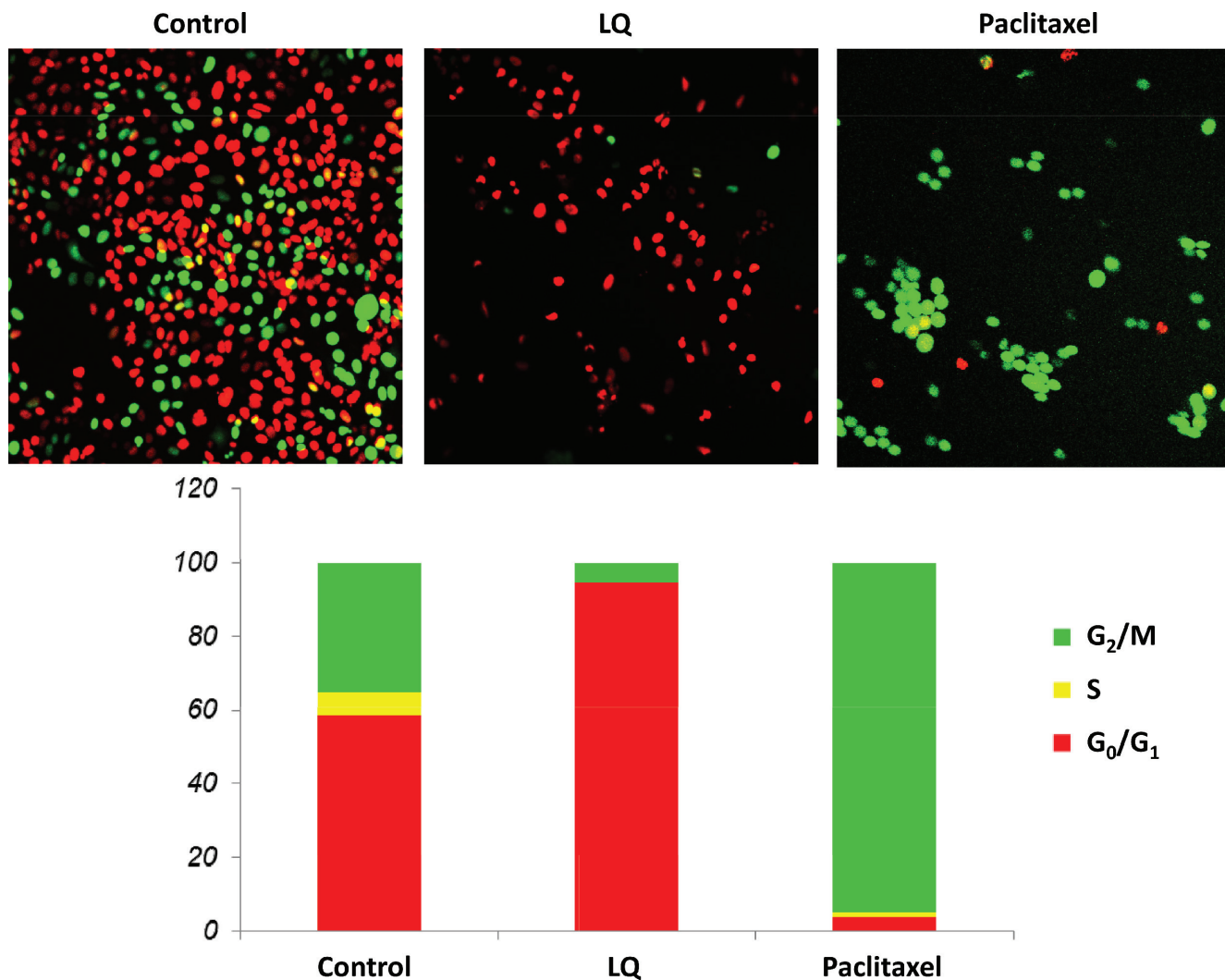


**Figure 1: LQ or paclitaxel treatment of Fucci-HeLa cells growing in 2D culture.** G<sub>0</sub>/G<sub>1</sub> arrest of HeLa Fucci cells was observed with LQ (9 mg/ml) treatment. Untreated control cells were distributed throughout the cell cycle. Paclitaxel was used as the positive control and resulted in an S/G<sub>2</sub>/M block. Bar graphs show the distribution of the cell-cycle phases with each treatment or control. See Materials and Methods for details.

24 hours. A pellet of HeLa-Fucci cells (10<sup>6</sup>) in 20~30  $\mu$ l DMEM supplemented with 10% fetal bovine serum, was gently placed on top of the Gelfoam<sup>®</sup>. Medium was added to the same height as the Gelfoam<sup>®</sup>.

#### Preparation of crude extracts of chinese herbs

LQ consists of a mixture of the following Chinese medicinal herbs: *Sinapis alba*, *Atractylodes macrocephala*, *Coix lacryma-jobi*, and *Polyporus adusta* (School of Pharmacy, Nanjing University of Traditional Chinese Medicine, Nanjing, China) as previously reported [30]. The ratio of the herbs used was (2:3:4:3). Dried plant parts used were: *Sinapis alba*, seed; *Atractylodes macrocephala*, root; *Coix lacryma-jobi*, kernel; *Polyporus adusta*, whole mushroom. Each herb was extracted in boiling water for

20 mins, the solution was filtered and the residue extracted with 75% ethanol when filtered. The water extract and ethanolic extract were combined and concentrated by lyophilization. The lyophilized powder was suspended in PBS and the mixture was vortexed for 1 min and incubated at 80°C for 30 min., cooled to room temperature, and was then centrifuged at 2000 rpm for 10 min. The supernatant was collected at a final concentration to 90 mg/ml and diluted and filtered through a 0.2  $\mu$ m membrane for *in vitro* use [31].

#### Chemotherapy drugs

Paclitaxel (Taxol) (Bedford Laboratories, Bedford, OH) was prepared by diluting to 0.2  $\mu$ M as a stock solution.

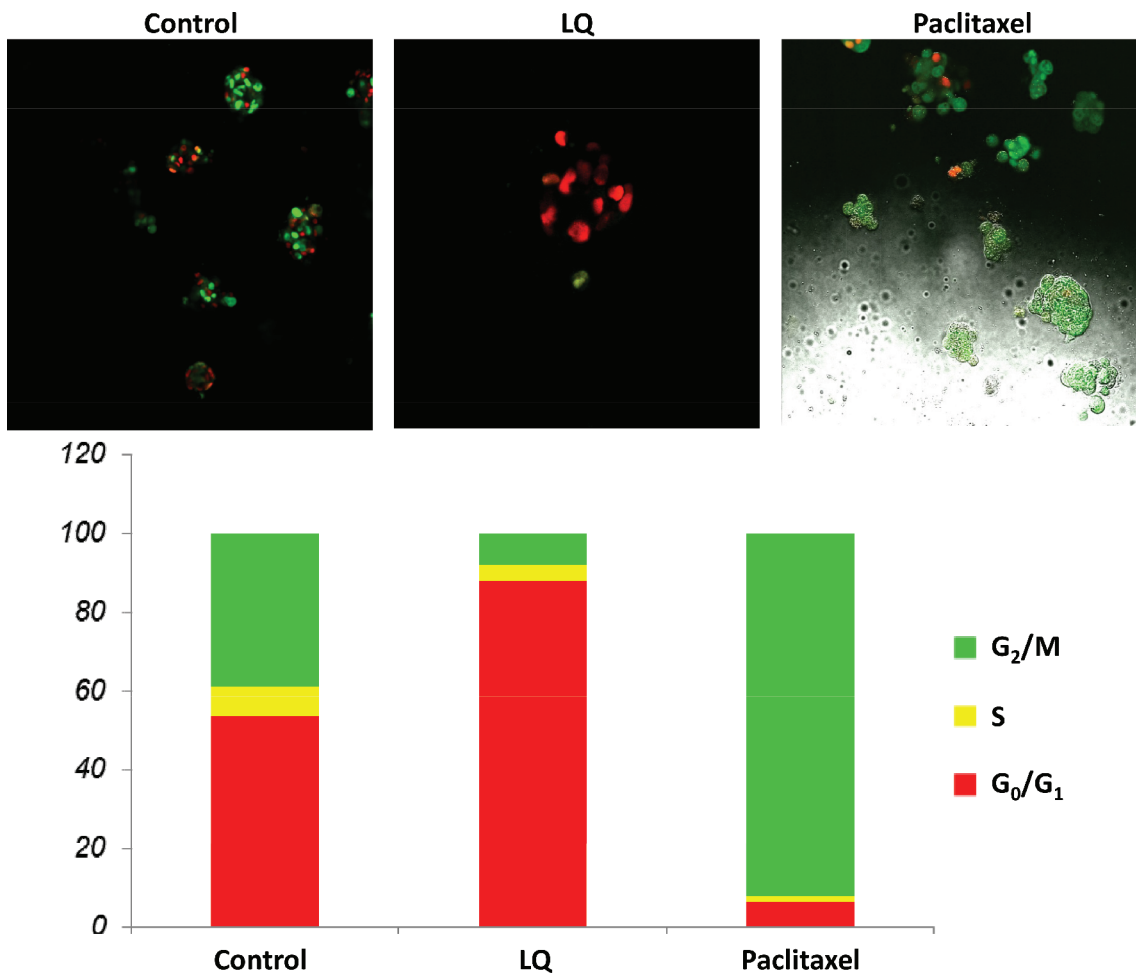


**Figure 2: LQ or paclitaxel treatment of FUCCI-HeLa cells growing in 2.5D Matrigel culture.** G<sub>0</sub>/G<sub>1</sub> arrest of HeLa-FUCCI cells was observed with LQ (9 mg/ml) treatment. Untreated control cells were distributed throughout the cell cycle. Paclitaxel was used as the positive control and resulted in an S/G<sub>2</sub>/M block. Bar graphs show the distribution of the cell-cycle phases. See Materials and Methods for details.

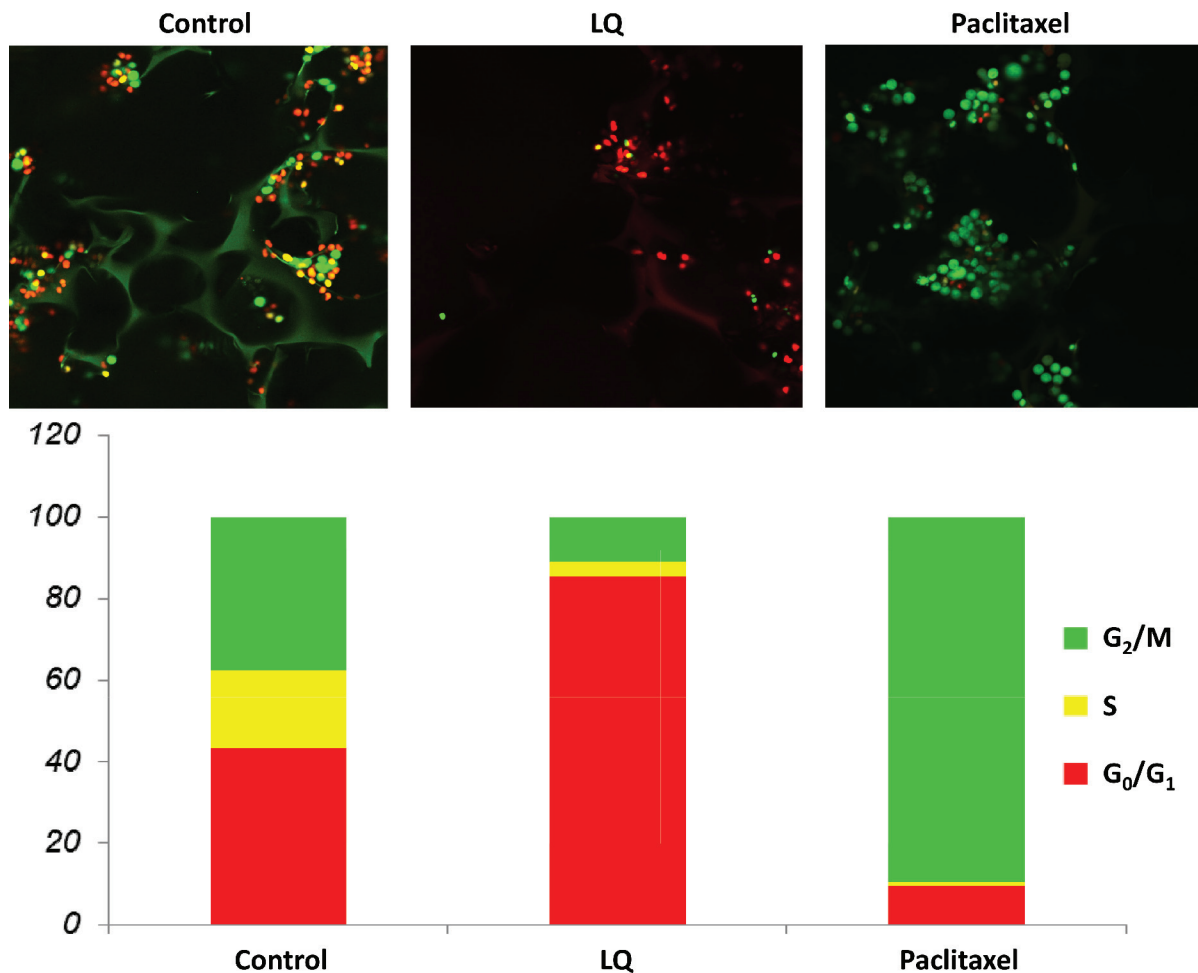


**Figure 3: LQ or paclitaxel treatment of FUCCI-HeLa cells growing in Gelfoam<sup>®</sup> histoculture.** G<sub>0</sub>/G<sub>1</sub> arrest of HeLa-FUCCI cells was observed with LQ (9 mg/ml) treatment. Untreated control cells were distributed throughout the cell cycle. Paclitaxel was used as the positive control and resulted in an S/G<sub>2</sub>/M block. Bar graphs show the distribution of the cell-cycle phases. See Materials and Methods for details.

### Imaging of FUCCI-expressing HeLa cells

Confocal laser scanning microscopy was performed with the FV1000 confocal laser scanning microscope (Olympus Corp., Tokyo, Japan) with 2 laser diodes (473 nm and 559 nm). A 4× (0.20 numerical aperture immersion) objective lens and a 20× (0.95 numerical aperture immersion) objective lens (Olympus) were used. Scanning and image acquisition were controlled by Fluoview software (Olympus). The tracing data were imported to Velocity 6.0 version (Perkin Elmer), where all 3D analysis was performed [32].

### Dedication

This paper is dedicated to the memory of A. R. Moossa, M.D.

### ACKNOWLEDGMENT

This study was supported in part by National Cancer Institute grant CA132971.

## Author contributions

Conceived and designed the experiments: LZ, CW, RMH. Performed the experiments: LZ, CW, SY. Analyzed the data: LZ, CW, MB, RMH. Contributed reagents/materials/analysis tools: CW, RMH. Wrote the manuscript: LZ, CW, RMH.

## REFERENCES

1. Zhang L, Wu C, Zhang Y, Liu F, Wang X, Zhao M, Hoffman RM. Comparison of efficacy and toxicity of Traditional Chinese Medicine (TCM) herbal mixture LQ and conventional chemotherapy on lung cancer metastasis and survival in mouse models. *PLoS One*. 2014; 9:e109814.
2. Zhang L, Wu C, Zhang Y, Liu F, Zhao M, Bouvet M, Hoffman RM. Efficacy comparison of traditional Chinese medicine LQ versus gemcitabine in a mouse model of pancreatic cancer. *J Cell Biochem*. 2013; 114:2131–2137.
3. Sakaue-Sawano A, Kurokawa H, Morimura T, Hanyu A, Hama H, Osawa H, Kashiwagi S, Fukami K, Miyata T, Miyoshi H, et al. Visualizing spatiotemporal dynamics of multicellular cell cycle progression. *Cell*. 2008; 132:487–98.
4. Yano S, Miwa S, Mii S, Hiroshima Y, Uehara F, Yamamoto M, Kishimoto H, Tazawa H, Bouvet M, Fujiwara T, Hoffman RM. Invading cancer cells are predominantly in G<sub>0</sub>/G<sub>1</sub> resulting in chemoresistance demonstrated by real-time FUCCI imaging. *Cell Cycle*. 2014; 13:953–960.
5. Yano S, Zhang Y, Miwa S, Tome Y, Hiroshima Y, Uehara F, Yamamoto M, Suetsugu A, Kishimoto H, Tazawa H, Zhao M, Bouvet M, Fujiwara T, Hoffman RM. Spatial-temporal FUCCI imaging of each cell in a tumor demonstrates locational dependence of cell cycle chemoresponsiveness. *Cell Cycle*. 2014; 13:2110–2119.
6. Hoffman RM, Jacobsen SJ. Reversible growth arrest in simian virus 40-transformed human fibroblasts. *Proc Natl Acad Sci USA*. 1980; 77:7306–7310.
7. Yano S, Li S, Han Q, Tan Y, Bouvet M, Fujiwara T, Hoffman RM. Selective methioninase-induced trap of cancer cells in S/G<sub>2</sub> phase visualized by FUCCI imaging confers chemosensitivity. *Oncotarget*. 2014; 5:8729–8736.
8. Wang X, Pan L, Mao N, Sun L, Qin X, Yin J. Cell-cycle synchronization reverses Taxol resistance of human ovarian cancer cell lines. *Cancer Cell Int*. 2013; 13:77.
9. Chandrasekaran B, Kute TE, Duch DS. Synchronization of cells in the S phase of the cell cycle by 3'-azido-3'-deoxythymidine: implications for cell cytotoxicity. *Cancer Chemother Pharmacol*. 1995; 35:489–495.
10. Kufe DW, Egan EM, Rosowsky A, Ensminger W, Frei E 3rd. Thymidine arrest and synchrony of cellular growth *in vivo*. *Cancer Treat Rep*. 1980; 64:1307–1317.
11. Keir ST, Friedman HS, Reardon DA, Bigner DD, Gray LA. Mibefradil, a novel therapy for glioblastoma multiforme: cell cycle synchronization and interlaced therapy in a murine model. *J Neurooncol*. 2013; 111:97–102.
12. Keyomarsi K, Sandoval L, Band V, Pardee AB. Synchronization of tumor and normal cells from G<sub>1</sub> to multiple cell cycles by lovastatin. *Cancer Res*. 1991; 51:3602–3609.
13. Javanmoghadam-Kamrani S, Keyomarsi K. Synchronization of the cell cycle using lovastatin. *Cell Cycle*. 2008; 7:2434–2440.
14. Vassilev LT. Cell cycle synchronization at the G<sub>2</sub>/M phase border by reversible inhibition of CDK1. *Cell Cycle*. 2006; 5:2555–2556.
15. Dong XF, Berthois Y, Dussert C, Isnardon D, Palmari J, Martin PM. Mode of EGF action on cell cycle kinetics in human breast cancer cell line MCF-7: some evidence that EGF acts as a “progression factor”. *Anticancer Res*. 1992; 12:2085–2092.
16. Hambek M, Werner C, Baghi M, Gstöttner W, Knecht R. Enhancement of docetaxel efficacy in head and neck cancer treatment by G<sub>0</sub> cell stimulation. *Eur J Cancer*. 2007; 43:1502–1507.
17. Hambek M, Werner C, Baghi M, Gstöttner W, Knecht R. Prestimulation of head and neck cancer cells with growth factors enhances treatment efficacy. *Anticancer Res*. 2006; 26:1091–1095.
18. Blagosklonny MV. How cancer could be cured by 2015. *Cell Cycle*. 2005; 4:269–278.
19. Blagosklonny MV. Tissue-selective therapy of cancer. *Br J Cancer*. 2003; 89:1147–1151.
20. Blagosklonny MV. Matching targets for selective cancer therapy. *Drug Discov Today*. 2003; 8:1104–1107.
21. Blagosklonny MV. “Targeting the absence” and therapeutic engineering for cancer therapy. *Cell Cycle*. 2008; 7:1307–1312.
22. Blagosklonny MV. Teratogens as anti-cancer drugs. *Cell Cycle*. 2005; 4:1518–1521.
23. Blagosklonny MV. Treatment with inhibitors of caspases, that are substrates of drug transporters, selectively permits chemotherapy-induced apoptosis in multidrug-resistant cells but protects normal cells. *Leukemia*. 2001; 15:936–941.
24. Blagosklonny MV. Target for cancer therapy: proliferating cells or stem cells. *Leukemia*. 2006; 20:385–391.
25. Blagosklonny MV. Cancer stem cell and cancer stemoids: from biology to therapy. *Cancer Biol Ther*. 2007; 6:1684–1690.
26. Apontes P, Leontieva OV, Demidenko ZN, Li F, Blagosklonny MV. Exploring long-term protection of normal human fibroblasts and epithelial cells from chemotherapy in cell culture. *Oncotarget*. 2011; 2:222–233.
27. Rao B, van Leeuwen IM, Higgins M, Campbell J, Thompson AM, Lane DP, Lain S. Evaluation of an Actinomycin D/VX-680 aurora kinase inhibitor combination in p53-based cyclotherapy. *Oncotarget*. 2010; 1:639–650.
28. Blagosklonny MV. NCI's provocative questions on cancer: some answers to ignite discussion. *Oncotarget*. 2011; 2:1352–1367.

29. Blagosklonny MV. Antagonistic drug combinations that select against drug resistance: from bacteria to cancer. *Cancer Biol Ther.* 2007; 6:1013–1014.
30. Zhang L, Wu C, Zhang Y, Liu F, Zhao M, Bouvet M, Hoffman RM. Efficacy comparison of traditional Chinese medicine LQ versus gemcitabine in a mouse model of pancreatic cancer. *J Cell Biochem.* 2013; 114:2131–2137.
31. Zhang L, Wu C, Zhang Y, Liu F, Wang X, Zhao M, Hoffman RM. Comparison of efficacy and toxicity of Traditional Chinese Medicine (TCM) herbal mixture LQ and conventional chemotherapy on lung cancer metastasis and survival in mouse models. *PLoS One.* 2014; 9:e109814.
32. Uchugonova A, Duong J, Zhang N, König K, Hoffman RM. The bulge area is the origin of nestin-expressing pluripotent stem cells of the hair follicle. *J Cell Biochem.* 2011; 112:2046–2050.